

Domain decomposition and adaptive sampling for physics-informed neural networks

Alexander Heinlein¹

Scientific Machine Learning: error control and analysis, Besançon, France, January 15-16, 2025

¹Delft University of Technology

Outline

1 FBPINNs – Multilevel domain decomposition-based architectures for physics-informed neural networks

Based on joint work with

Victorita Dolean

(Eindhoven University of Technology)

Ben Moseley and Siddhartha Mishra

(ETH Zürich)

2 Stacking multifidelity physics-informed neural networks

Based on joint work with

Damien Beecroft

(University of Washington)

Amanda A. Howard and Panos Stinis

(Pacific Northwest National Laboratory)

3 Multilevel domain decomposition-based physics-informed deep operator networks

Based on joint work with

Amanda A. Howard and Panos Stinis

(Pacific Northwest National Laboratory)

4 PACMANN – Point adaptive collocation method for artificial neural networks

Based on joint work with

Bianca Giovanardi and Coen Visser

(Delft University of Technology)

FBPINNs – Multilevel domain decomposition-based architectures for physics-informed neural networks

Physics-Informed Neural Networks (PINNs)

In the physics-informed neural network (PINN) approach introduced by [Raissi et al. \(2019\)](#), a neural network is employed to discretize a partial differential equation

$$\mathcal{N}[u] = f, \quad \text{in } \Omega.$$

PINNs use a **hybrid loss function**:

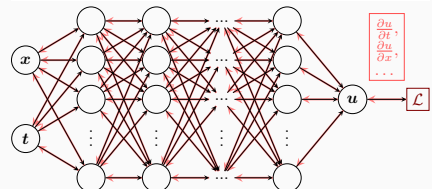
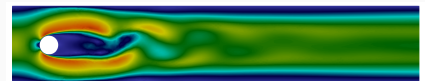
$$\mathcal{L}(\theta) = \omega_{\text{data}} \mathcal{L}_{\text{data}}(\theta) + \omega_{\text{PDE}} \mathcal{L}_{\text{PDE}}(\theta),$$

where ω_{data} and ω_{PDE} are **weights** and

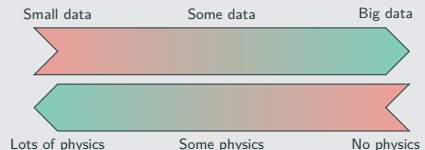
$$\mathcal{L}_{\text{data}}(\theta) = \frac{1}{N_{\text{data}}} \sum_{i=1}^{N_{\text{data}}} (u(\hat{x}_i, \theta) - u_i)^2,$$

$$\mathcal{L}_{\text{PDE}}(\theta) = \frac{1}{N_{\text{PDE}}} \sum_{i=1}^{N_{\text{PDE}}} (\mathcal{N}[u](x_i, \theta) - f(x_i))^2.$$

See also [Dissanayake and Phan-Thien \(1994\)](#); [Lagaris et al. \(1998\)](#).



Hybrid loss



Advantages

- "Meshfree"
- Small data
- Generalization properties
- High-dimensional problems
- Inverse and parameterized problems

Drawbacks

- Training cost and robustness
- Convergence not well-understood
- Difficulties with scalability and multi-scale problems

- Known solution values can be included in $\mathcal{L}_{\text{data}}$
- Initial and boundary conditions are also included in $\mathcal{L}_{\text{data}}$

Theoretical Result for PINNs

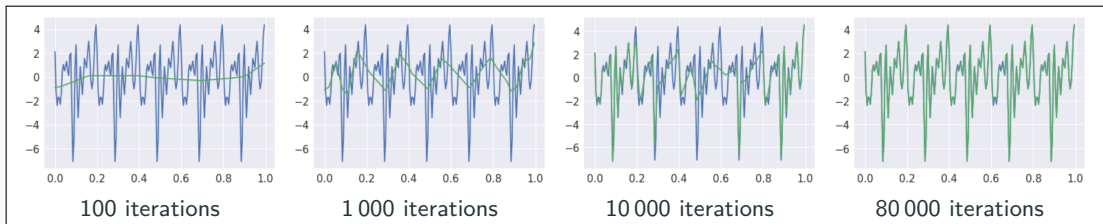
Estimate of the generalization error (Mishra and Molinaro (2022))

The generalization error (or total error) satisfies

$$\mathcal{E}_G \leq C_{\text{PDE}} \mathcal{E}_{\mathcal{T}} + C_{\text{PDE}} C_{\text{quad}}^{1/p} N^{-\alpha/p}$$

- $\mathcal{E}_G = \mathcal{E}_G(\mathbf{X}, \theta) := \|\mathbf{u} - \mathbf{u}^*\|_V$ **general. error** (V Sobolev space, \mathbf{X} training data set)
- $\mathcal{E}_{\mathcal{T}}$ **training error** (l^p loss of the residual of the PDE)
- N **number of the training points** and α **convergence rate of the quadrature**
- C_{PDE} and C_{quad} **constants** depending on the **PDE, quadrature, and neural network**

Rule of thumb: “As long as the PINN is **trained well**, it also **generalizes well**”



Rahaman et al., *On the spectral bias of neural networks*, ICML (2019)

Motivation – Some Observations on the Performance of PINNs

Solve

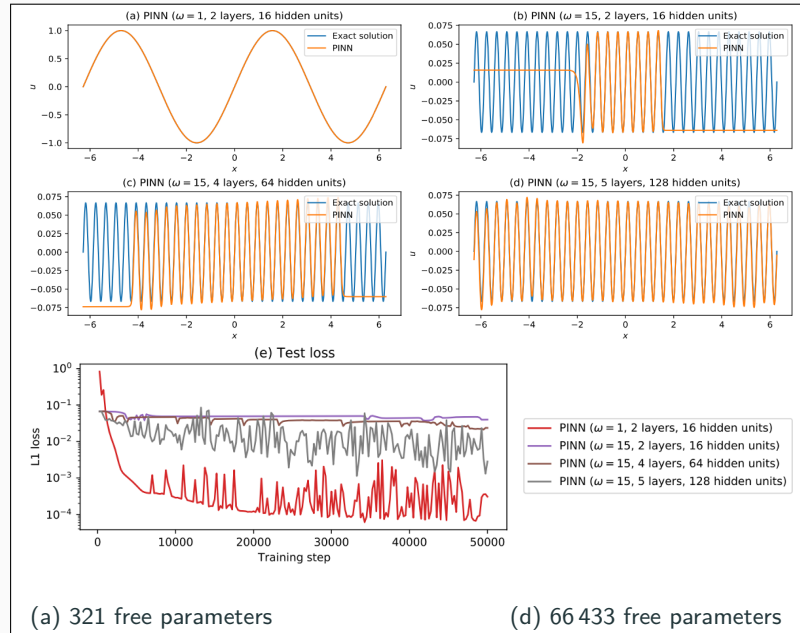
$$\begin{aligned} u' &= \cos(\omega x), \\ u(0) &= 0, \end{aligned}$$

for different values of ω
using PINNs with
varying network
capacities.

Scaling issues

- Large computational domains
- Small frequencies

Cf. Moseley, Markham, and
Nissen-Meyer (2023)



Motivation – Some Observations on the Performance of PINNs

Solve

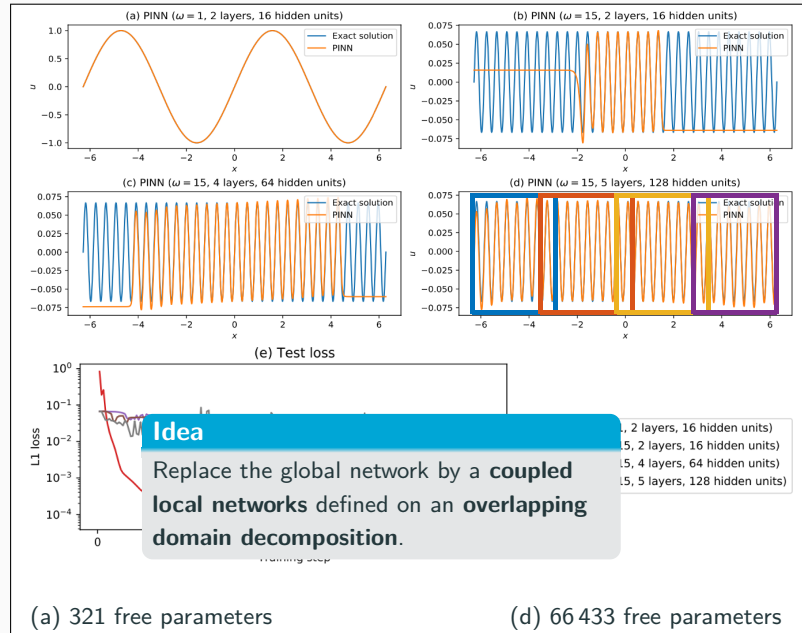
$$\begin{aligned} u' &= \cos(\omega x), \\ u(0) &= 0, \end{aligned}$$

for different values of ω
using PINNs with
varying network
capacities.

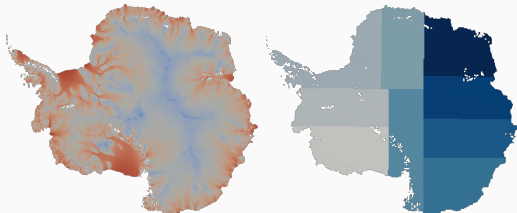
Scaling issues

- Large computational domains
- Small frequencies

Cf. Moseley, Markham, and Nissen-Meyer (2023)



Domain Decomposition Methods



Images based on Heinlein, Perego, Rajamanickam (2022)

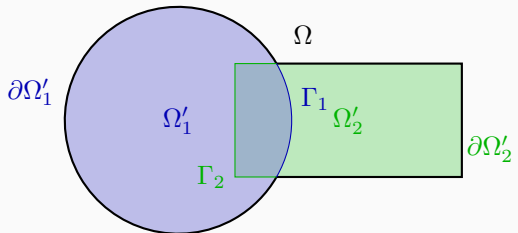
Historical remarks: The **alternating Schwarz method** is the earliest **domain decomposition method (DDM)**, which has been invented by **H. A. Schwarz** and published in **1870**:

- Schwarz used the algorithm to establish the **existence of harmonic functions** with prescribed boundary values on **regions with non-smooth boundaries**.

Idea

Decomposing a large **global problem** into smaller **local problems**:

- Better robustness** and **scalability** of numerical solvers
- Improved computational efficiency**
- Introduce **parallelism**

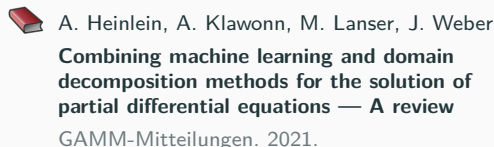


Domain Decomposition Methods and Machine Learning – Literature

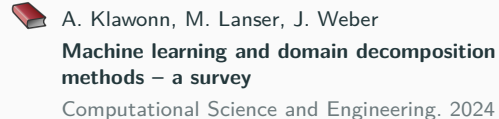
A non-exhaustive literature overview:

- Machine Learning for adaptive BDDC, FETI–DP, and AGDSW: Heinlein, Klawonn, Lanser, Weber (2019, 2020, 2021, 2021, 2021, 2022); Klawonn, Lanser, Weber (2024)
- cPINNs, XPINNs: Jagtap, Kharazmi, Karniadakis (2020); Jagtap, Karniadakis (2020)
- Classical Schwarz iteration for PINNs or DeepRitz (D3M, DeepDDM, etc):: Li, Tang, Wu, and Liao (2019); Li, Xiang, Xu (2020); Mercier, Gratton, Boudier (arXiv 2021); Dolean, Heinlein, Mercier, Gratton (subm. 2024 / arXiv:2408.12198); Li, Wang, Cui, Xiang, Xu (2023); Sun, Xu, Yi (arXiv 2023, 2024); Kim, Yang (2023, 2024, 2024)
- FBPINNs, FBKANs: Moseley, Markham, and Nissen-Meyer (2023); Dolean, Heinlein, Mishra, Moseley (2024, 2024); Heinlein, Howard, Beecroft, Stinis (acc. 2024 / arXiv:2401.07888); Howard, Jacob, Murphy, Heinlein, Stinis (arXiv:2406.19662)
- DDMs for CNNs: Gu, Zhang, Liu, Cai (2022); Lee, Park, Lee (2022); Klawonn, Lanser, Weber (2024); Verburg, Heinlein, Cyr (subm. 2024)

An overview of the state-of-the-art in early 2021:



An overview of the state-of-the-art in mid 2024:



Finite Basis Physics-Informed Neural Networks (FBPINNs)

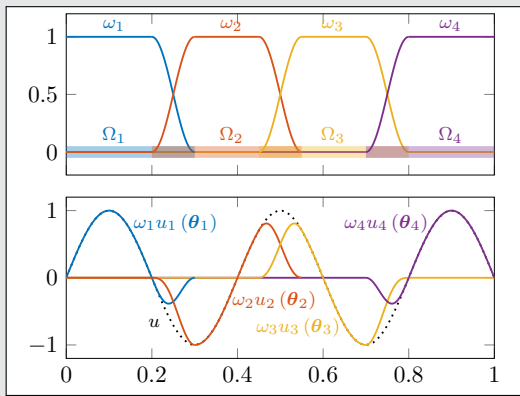
FBPINNs ([Moseley, Markham, Nissen-Meyer \(2023\)](#))

FBPINNs employ the **network architecture**

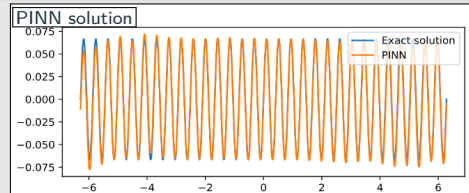
$$u(\theta_1, \dots, \theta_J) = \sum_{j=1}^J \omega_j u_j(\theta_j)$$

and the **loss function**

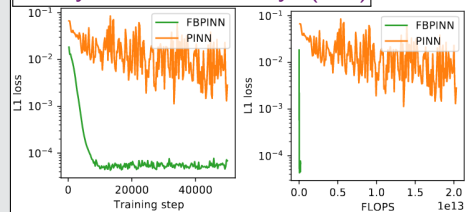
$$\mathcal{L} = \frac{1}{N} \sum_{i=1}^N \left(n \left[\sum_{x_i \in \Omega_j} \omega_j u_j(x_i, \theta_j) \right] - f(x_i) \right)^2$$



1D single-frequency problem



[Moseley, Markham, Nissen-Meyer \(2023\)](#)



Finite Basis Physics-Informed Neural Networks (FBPINNs)

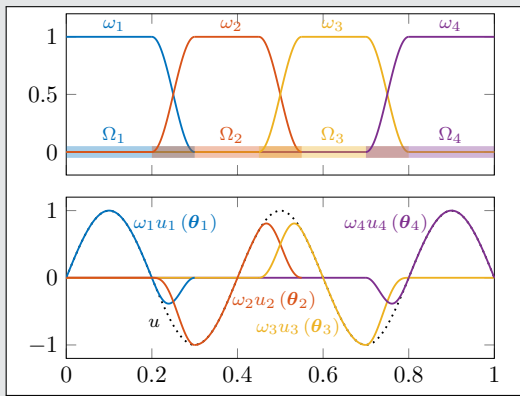
FBPINNs ([Moseley, Markham, Nissen-Meyer \(2023\)](#))

FBPINNs employ the **network architecture**

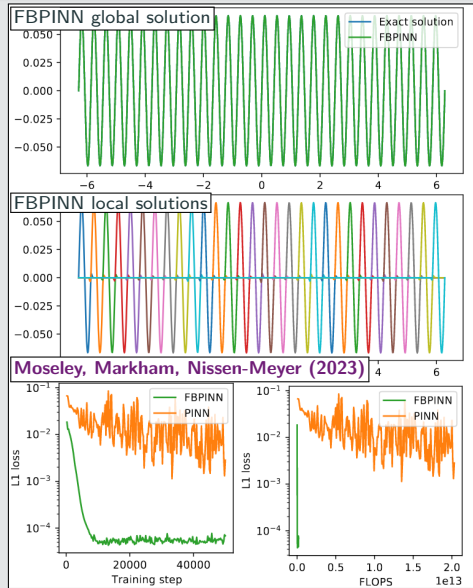
$$u(\theta_1, \dots, \theta_J) = \sum_{j=1}^J \omega_j u_j(\theta_j)$$

and the **loss function**

$$\mathcal{L} = \frac{1}{N} \sum_{i=1}^N \left(n \left[\sum_{x_i \in \Omega_j} \omega_j u_j(x_i, \theta_j) \right] - f(x_i) \right)^2$$



1D single-frequency problem



Finite Basis Physics-Informed Neural Networks (FBPINNs)

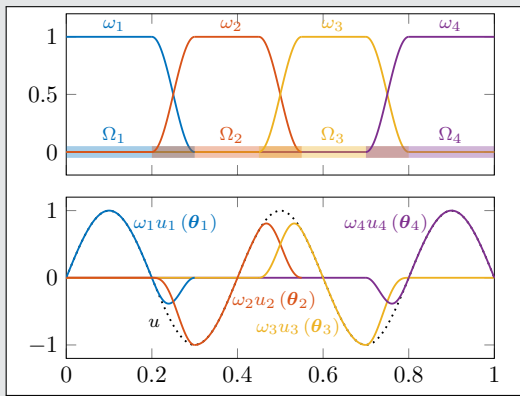
FBPINNs ([Moseley, Markham, Nissen-Meyer \(2023\)](#))

FBPINNs employ the **network architecture**

$$u(\theta_1, \dots, \theta_J) = \sum_{j=1}^J \omega_j u_j(\theta_j)$$

and the **loss function**

$$\mathcal{L} = \frac{1}{N} \sum_{i=1}^N \left(n \left[\sum_{x_i \in \Omega_j} \omega_j u_j(x_i, \theta_j) - f(x_i) \right] \right)^2$$



Scalability of FBPINNs

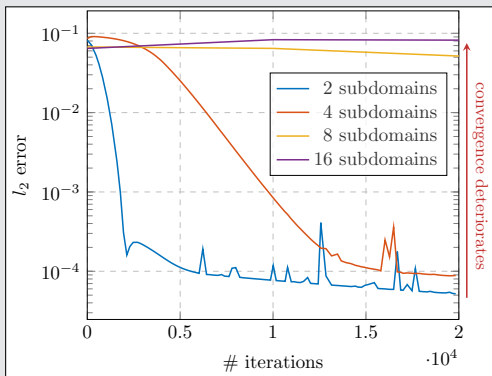
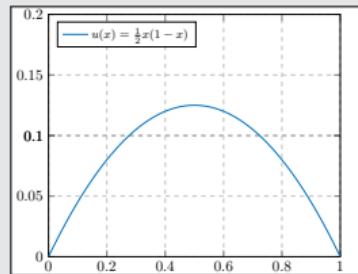
Consider the simple boundary value problem

$$-u'' = 1 \text{ in } [0, 1],$$

$$u(0) = u(1) = 0,$$

which has the **solution**

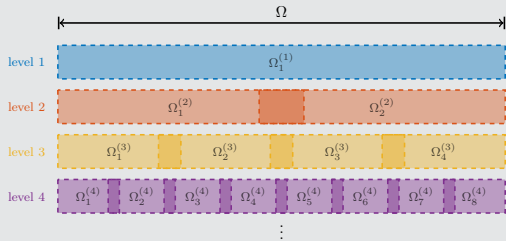
$$u(x) = \frac{1}{2}x(1-x).$$



Numerical Results for FBPINNs

Multi-level FBPINNs (ML-FBPINNs)

ML-FBPINNs (Dolean, Heinlein, Mishra, Moseley (2024)) are based on a **hierarchy of domain decompositions**:



This yields the **network architecture**

$$u(\theta_1^{(1)}, \dots, \theta_{J^{(L)}}^{(L)}) = \sum_{l=1}^L \sum_{j=1}^{N^{(l)}} \omega_j^{(l)} u_j^{(l)}(\theta_j^{(l)})$$

and the **loss function**

$$\mathcal{L} = \frac{1}{N} \sum_{i=1}^N \left(n \left[\sum_{x_i \in \Omega_j^{(l)}} \omega_j^{(l)} u_j^{(l)}(x_i, \theta_j^{(l)}) - f(x_i) \right]^2 \right)$$

Multi-Frequency Problem

Let us now consider the two-dimensional multi-frequency Laplace boundary value problem

$$-\Delta u = 2 \sum_{i=1}^n (\omega_i \pi)^2 \sin(\omega_i \pi x) \sin(\omega_i \pi y) \quad \text{in } \Omega,$$

$$u = 0 \quad \text{on } \partial\Omega,$$

$$\text{with } \omega_i = 2^i.$$

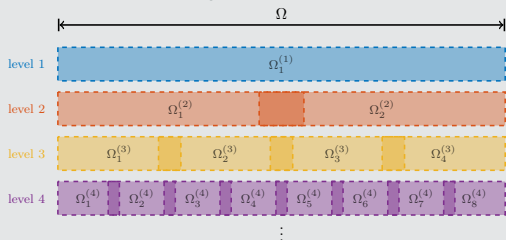
For increasing values of n , we obtain the analytical solutions:



Numerical Results for FBPINNs

Multi-level FBPINNs (ML-FBPINNs)

ML-FBPINNs (Dolean, Heinlein, Mishra, Moseley (2024)) are based on a **hierarchy of domain decompositions**:



This yields the **network architecture**

$$u(\theta_1^{(1)}, \dots, \theta_{J^{(L)}}^{(L)}) = \sum_{l=1}^L \sum_{j=1}^{N^{(l)}} \omega_j^{(l)} u_j^{(l)}(\theta_j^{(l)})$$

and the **loss function**

$$\mathcal{L} = \frac{1}{N} \sum_{i=1}^N \left(n \left[\sum_{x_i \in \Omega_j^{(l)}} \omega_j^{(l)} u_j^{(l)} \right] (\mathbf{x}_i, \theta_j^{(l)}) - f(\mathbf{x}_i) \right)^2$$

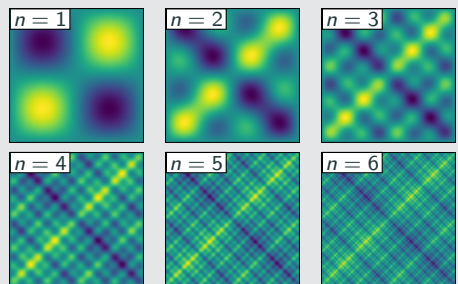
Multi-Frequency Problem

Let us now consider the **two-dimensional multi-frequency Laplace boundary value problem**

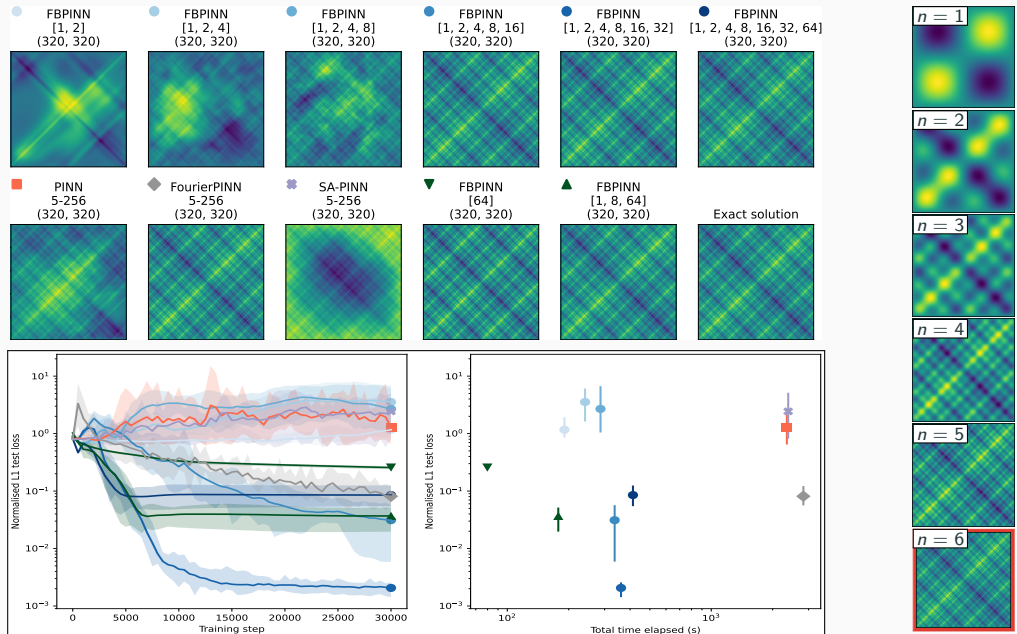
$$-\Delta u = 2 \sum_{i=1}^n (\omega_i \pi)^2 \sin(\omega_i \pi x) \sin(\omega_i \pi y) \quad \text{in } \Omega,$$
$$u = 0 \quad \text{on } \partial\Omega,$$

with $\omega_i = 2^i$.

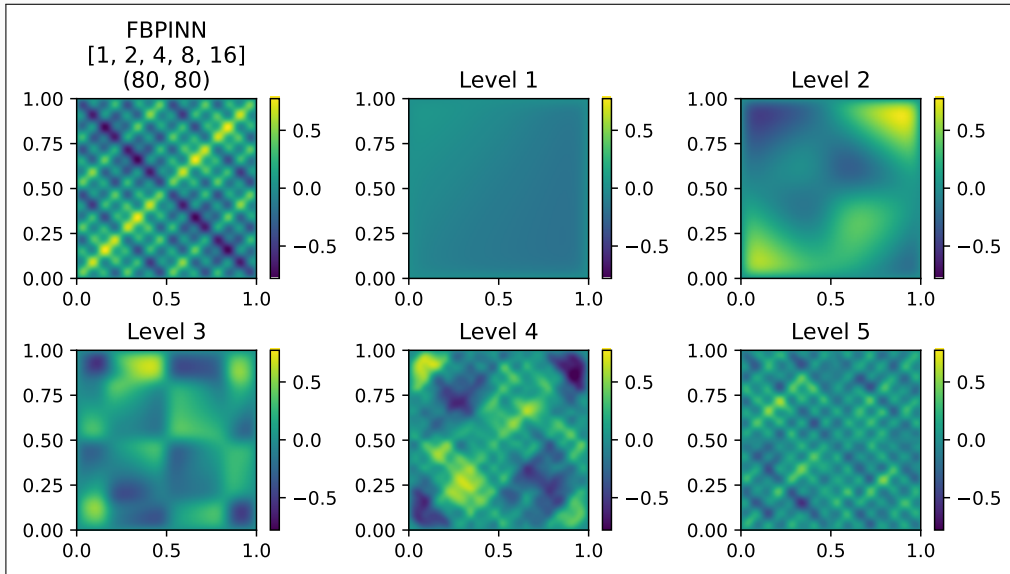
For increasing values of n , we obtain the **analytical solutions**:



Multi-Level FBPINNs for a Multi-Frequency Problem – Strong Scaling

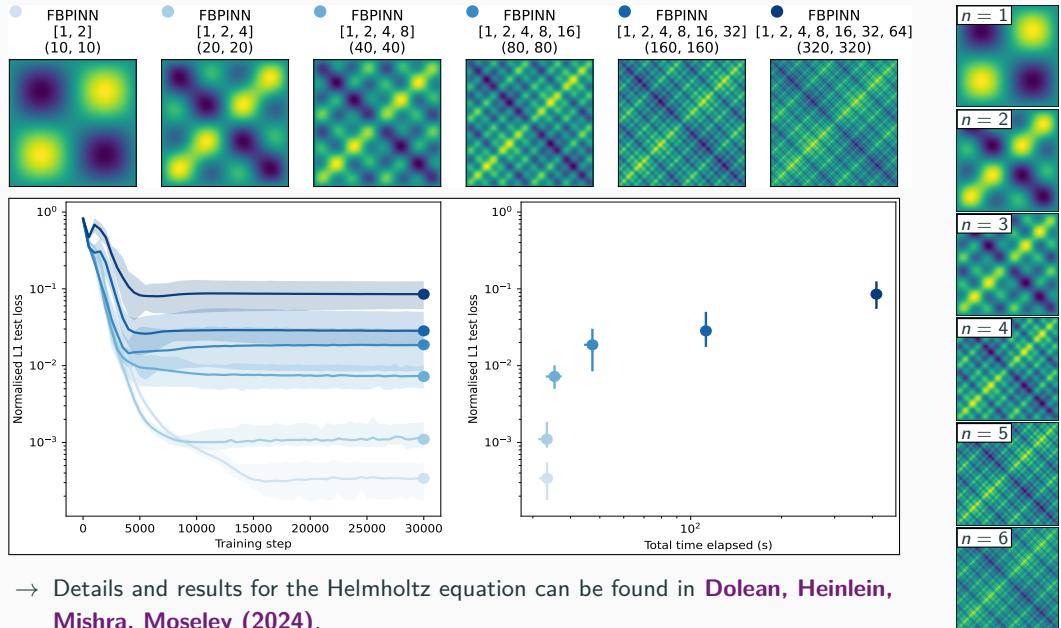


Multi-Frequency Problem – What the FBPINN Learns



Cf. Dolean, Heinlein, Mishra, Moseley (2024).

Multi-Level FBPINNs for a Multi-Frequency Problem – Weak Scaling



→ Details and results for the Helmholtz equation can be found in **Dolean, Heinlein, Mishra, Moseley (2024)**.

Stacking multifidelity physics-informed neural networks

PINNs for Time-Dependent Problems

We investigate the performance of PINNs for time-dependent problems. Therefore, consider the simple **pendulum problem**:

$$\frac{ds_1}{dt} = s_2,$$

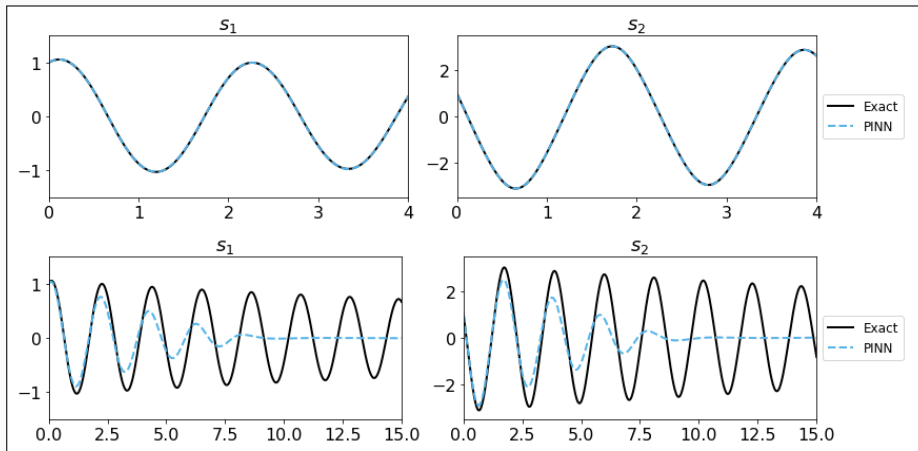
$$\frac{ds_2}{dt} = -\frac{b}{m}s_2 - \frac{g}{L} \sin(s_1).$$

Problem parameters

$$m = L = 1, b = 0.05,$$

$$g = 9.81$$

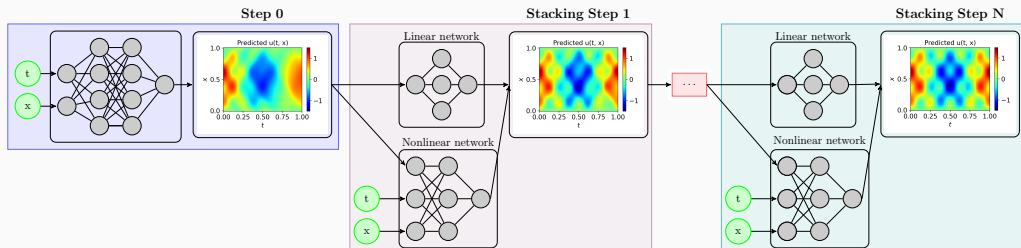
- **Top:** $T = 4$
- **Bottom:** $T = 20$



Stacking Multifidelity PINNs

In the **stacking multifidelity PINNs approach** introduced in [Howard, Murphy, Ahmed, Stinis \(arXiv 2023\)](#), multiple PINNs are trained in a recursive way. In each step, a model u^{MF} is trained based on the previous model u^{SF} :

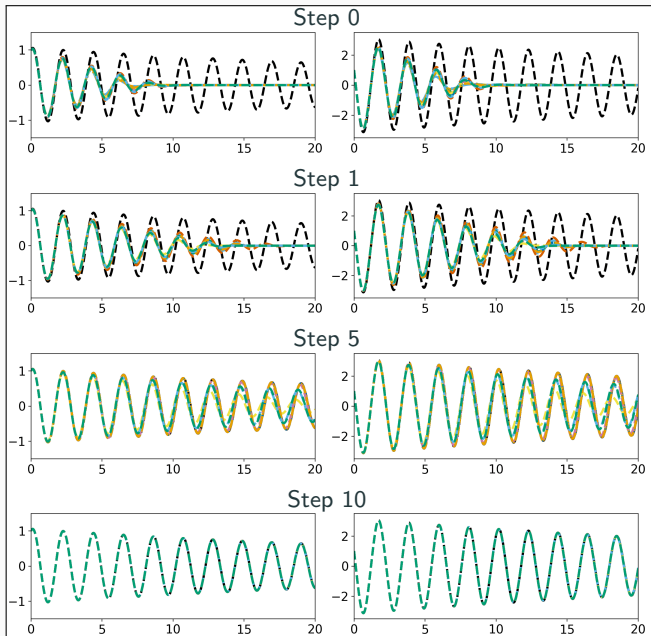
$$u^{MF}(x, \theta^{MF}) = (1 - |\alpha|) u_{\text{linear}}^{MF}(x, \theta^{MF}, u^{SF}) + |\alpha| u_{\text{nonlinear}}^{MF}(x, \theta^{MF}, u^{SF})$$



Related works (non-exhaustive list)

- Cokriging & multifidelity Gaussian process regression: E.g., [Wackernagel \(1995\)](#); [Perdikaris et al. \(2017\)](#); [Babaei et al. \(2020\)](#)
- Multifidelity PINNs & DeepONet: [Meng and Karniadakis \(2020\)](#); [Howard, Fu, and Stinis \(2024\)](#); [Howard, Perego, Karniadakis, Stinis \(2023\)](#); [Howard, Murphy, Ahmed, Stinis \(arXiv 2023\)](#)
- Galerkin, multi-level, and multi-stage neural networks: [Ainsworth and Dong \(2021\)](#); [Ainsworth and Dong \(2022\)](#); [Aldirany et al. \(2024\)](#); [Wang and Lai \(2024\)](#)

Stacking Multifidelity PINNs for the Pendulum Problem

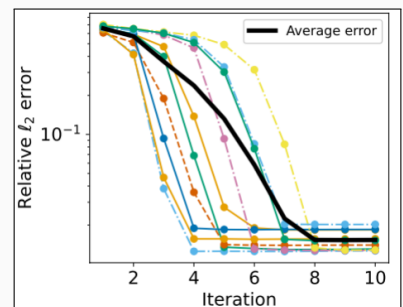


Pendulum problem:

$$\frac{d\beta_1}{dt} = \beta_2,$$

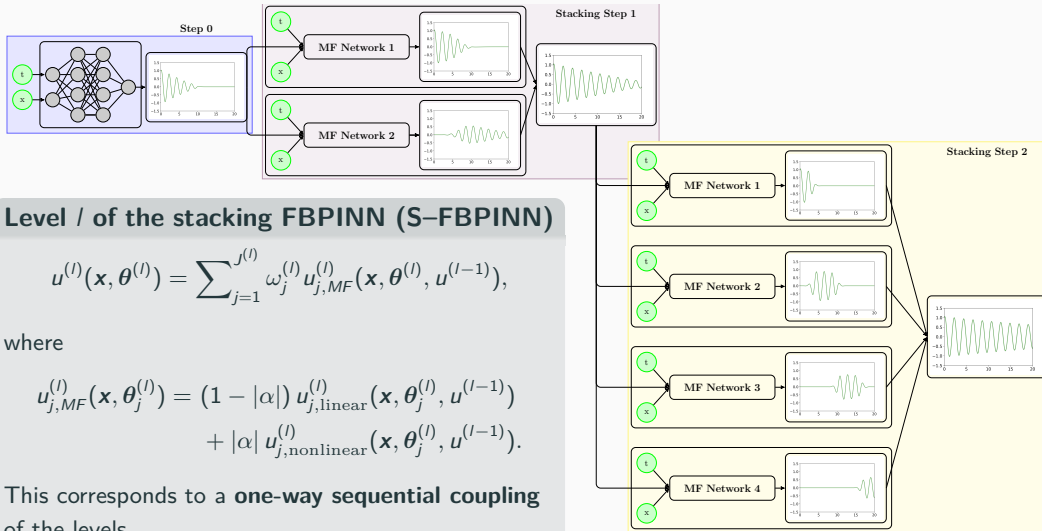
$$\frac{d\beta_2}{dt} = -\frac{b}{m}\beta_2 - \frac{g}{L} \sin(\beta_1).$$

with $m = L = 1$, $b = 0.05$, $g = 9.81$,
and $T = 20$.



Stacking Multifidelity FBPINNs

In Heinlein, Howard, Beecroft, and Stinis (acc. 2024 / arXiv:2401.07888), we **combine stacking multifidelity PINNs with FBPINNs** by using an FBPINN model in each stacking step.



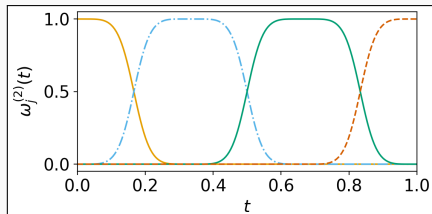
Numerical Results – Pendulum Problem

First, we consider a pendulum problem and compare the stacking multifidelity PINN and FBPINN approaches:

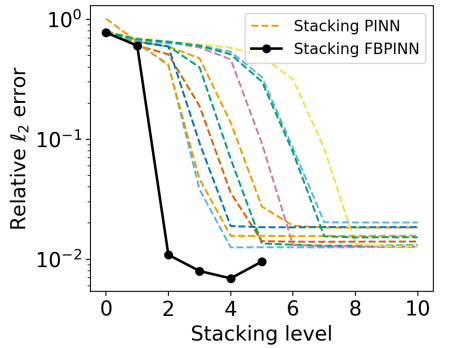
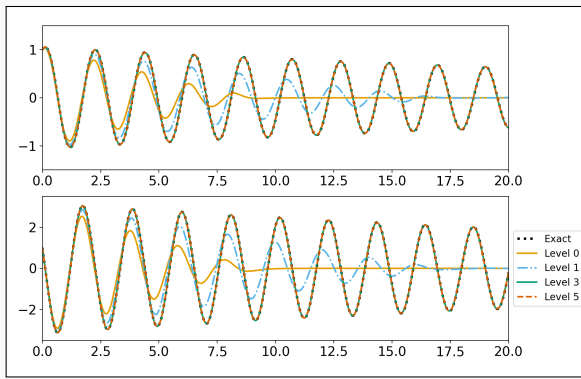
$$\frac{d\beta_1}{dt} = \beta_2,$$

$$\frac{d\beta_2}{dt} = -\frac{b}{m}\beta_2 - \frac{g}{L} \sin(\beta_1)$$

with $m = L = 1$, $b = 0.05$, $g = 9.81$, and $T = 20$.



Exemplary partition of unity in time



Numerical Results – Pendulum Problem

First, we consider a pendulum problem and compare the stacking multifidelity PINN and FBPINN approaches:

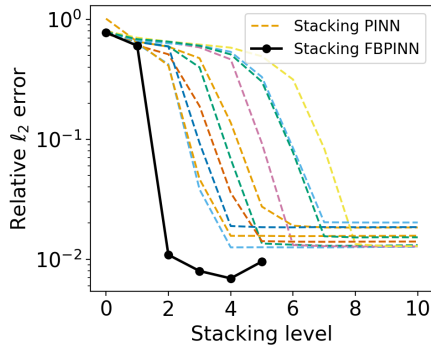
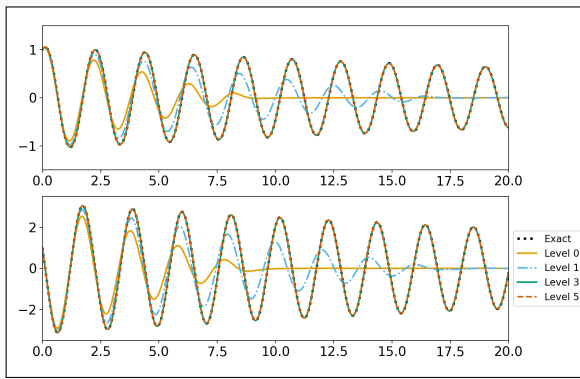
$$\frac{d\beta_1}{dt} = \beta_2,$$

$$\frac{d\beta_2}{dt} = -\frac{b}{m}\beta_2 - \frac{g}{L} \sin(\beta_1)$$

with $m = L = 1$, $b = 0.05$, $g = 9.81$, and $T = 20$.

Model details:

method	arch.	# levels	# params	error
S-PINN	5x50, 1x20	4	63 018	0.0125
S-FBPINN	3x32, 1x 4	2	34 570	0.0074



Numerical Results – Two-Frequency Problem

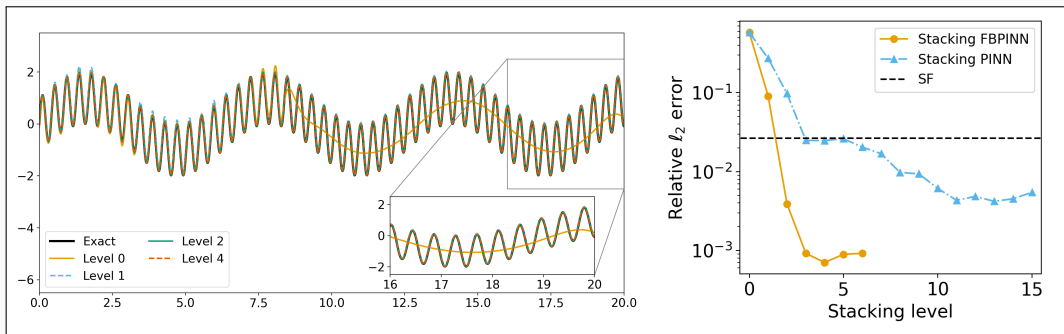
Second, we consider a **two-frequency problem**:

$$\frac{ds}{dx} = \omega_1 \cos(\omega_1 x) + \omega_2 \cos(\omega_2 x),$$

$$s(0) = 0,$$

on domain $\Omega = [0, 20]$ with $\omega_1 = 1$ and $\omega_2 = 15$.

method	arch.	# levels	# params	error
PINN	4x64	0	12 673	0.6543
PINN	5x64	0	16 833	0.0265
S-PINN	4x16, 1x5	3	4900	0.0249
S-PINN	4x16, 1x5	10	11 179	0.0061
S-FBPINN	4x16, 1x5	2	7822	0.00415
S-FBPINN	4x16, 1x5	5	59 902	0.00083

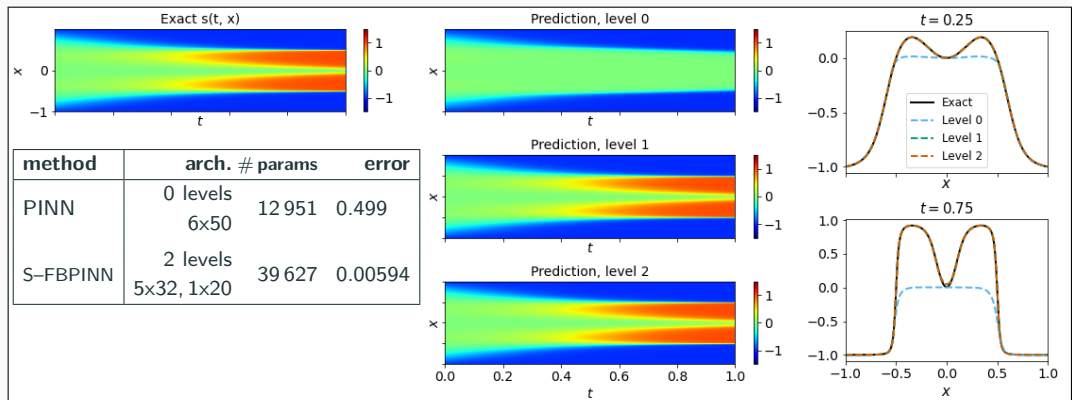


→ Due to the **multiscale structure of the problem**, the **improvements** due to the **multipidelity FBPINN approach** are **even stronger**.

Numerical Results – Allen–Cahn Equation

Finally, we consider the **Allen–Cahn equation**:

$$\begin{aligned}\vartheta_t - 0.0001\vartheta_{xx} + 5\vartheta^3 - 5\vartheta &= 0, & t \in (0, 1], x \in [-1, 1], \\ \vartheta(x, 0) &= x^2 \cos(\pi x), & x \in [-1, 1], \\ \vartheta(x, t) &= \vartheta(-x, t), & t \in [0, 1], x = -1, x = 1, \\ \vartheta_x(x, t) &= \vartheta_x(-x, t), & t \in [0, 1], x = -1, x = 1.\end{aligned}$$



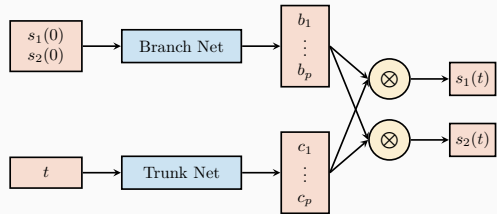
PINN gets stuck at fixed point of the dynamical system; cf. [Rohrhofer et al. \(arXiv 2023\)](#).

Multilevel domain decomposition-based physics-informed deep operator networks

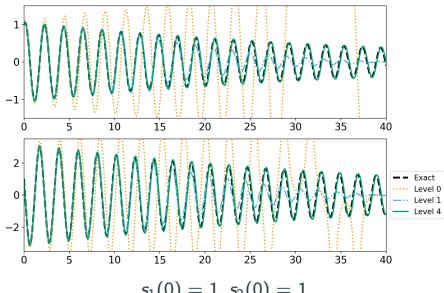
Deep Operator Networks (DeepONets / DONs)

DeepONets (Lu et al. (2021))

- While PINNs learn individual solutions, neural operators learn operators between function spaces, such as **solution operators**
- Deep operator networks (DeepONets)** are compatible with the PINN approach but **physics-informed DeepONets (PI-DONs)** are challenging to train

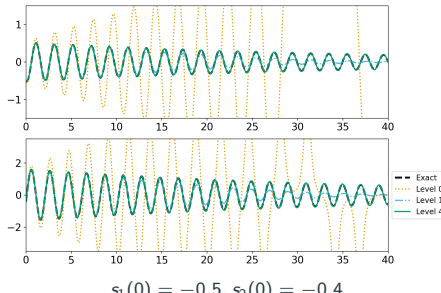


Approach based on the **single-layer case** analyzed in **Chen and Chen (1995)**



$s_1(0) = 1, s_2(0) = 1$

Cf. Heinlein, Howard, Beecroft, and Stinis (acc. 2024).

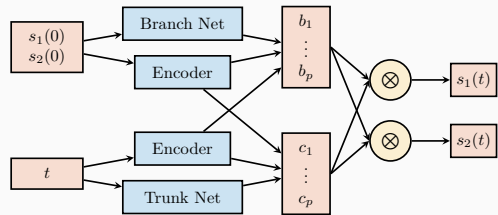


$s_1(0) = -0.5, s_2(0) = -0.4$

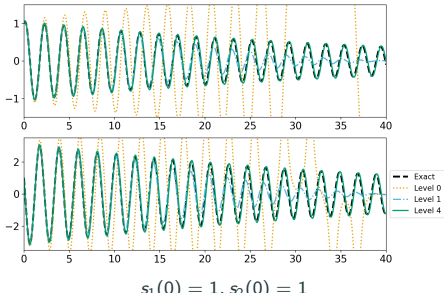
Deep Operator Networks (DeepONets / DONs)

DeepONets (Lu et al. (2021))

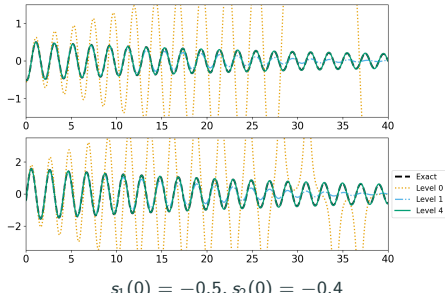
- While PINNs learn individual solutions, neural operators learn operators between function spaces, such as **solution operators**
- **Deep operator networks (DeepONets)** are compatible with the PINN approach but **physics-informed DeepONets (PI-DONs)** are challenging to train



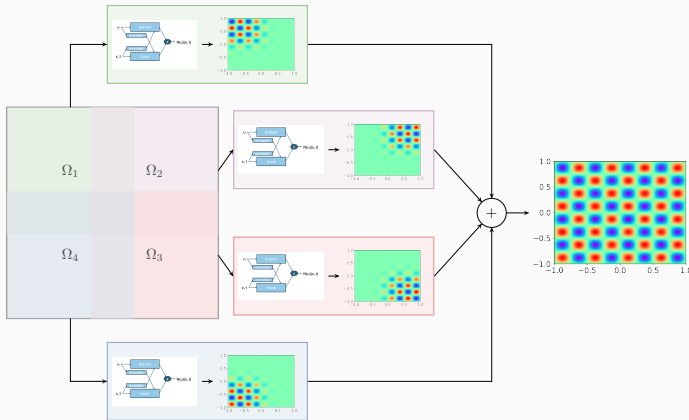
Modified DeepONet architecture; cf. **Wang, Wang, and Perdikaris (2022)**



Cf. **Heinlein, Howard, Beecroft, and Stinis (acc. 2024)**.



Finite Basis DeepONets (FBDONs)



Howard, Heinlein, Stinis (in prep.)

Variants:

Shared-trunk FBDONs (ST-FBDONs)

The trunk net learns spatio-temporal basis functions. In ST-FBDONs, we use the same trunk network for all subdomains.

Stacking FBDONs

Combination of the stacking multifidelity approach with FBDONs.

Heinlein, Howard, Beecroft, Stinis (acc. 2024/arXiv:2401.07888)

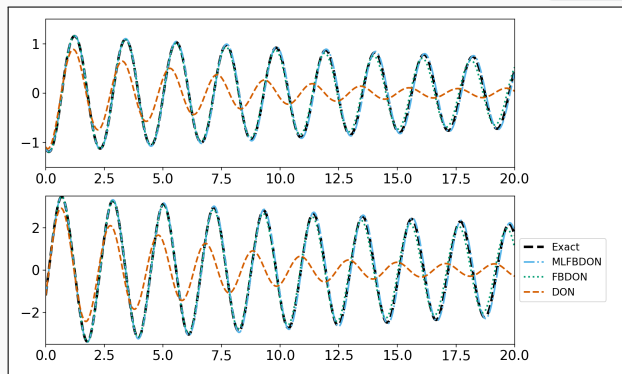
DD-DONs Pendulum

Pendulum problem

$$\frac{ds_1}{dt} = s_2, \quad t \in [0, T],$$

$$\frac{ds_2}{dt} = -\frac{b}{m}s_2 - \frac{g}{L} \sin(s_1), \quad t \in [0, T],$$

where $m = L = 1$, $b = 0.05$, $g = 9.81$, and $T = 20$.



Parametrization

Initial conditions:

$$s_1(0) \in [-2, 2] \quad s_2(0) \in [-1.2, 1.2]$$

$s_1(0)$ and $s_2(0)$ are also inputs of the branch network.

Training on 50 k different configurations

Mean rel. l_2 error on 100 config.

DeepONet	0.94
FBDON (32 subd.)	0.84
MLFBDON ([1, 4, 8, 16, 32] subd.)	0.27

Cf. [Howard, Heinlein, Stinis \(in prep.\)](#)

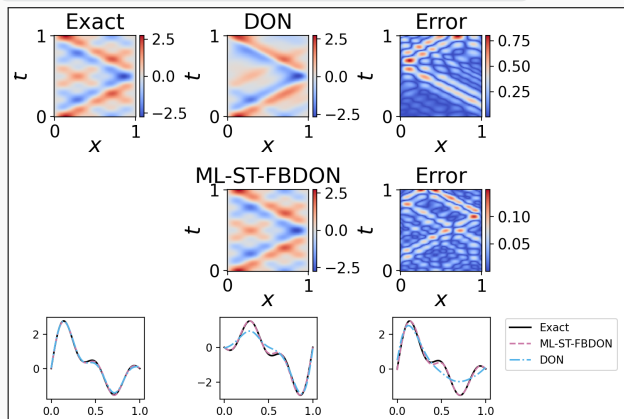
DD-DONs Wave Equation

Wave equation

$$\frac{d^2s}{dt^2} = 2 \frac{d^2s}{dx^2}, \quad (x, t) \in [0, 1]^2$$

$$s_t(x, 0) = 0, x \in [0, 1], \quad s(0, t) = s(1, t) = 0,$$

Solution: $s(x, t) = \sum_{n=1}^5 b_n \sin(n\pi x) \cos(n\pi\sqrt{2}t)$



Parametrization

Initial conditions for s parametrized by $b = (b_1, \dots, b_5)$ (normally distributed):

$$s(x, 0) = \sum_{n=1}^5 b_n \sin(n\pi x) \quad x \in [0, 1]$$

Training on 1000 random configurations.

Mean rel. ℓ_2 error on 100 config.

DeepONet	0.30 ± 0.11
ML-ST-FBDON ([1, 4, 8, 16] subd.)	0.05 ± 0.03
ML-FBDON ([1, 4, 8, 16] subd.)	0.08 ± 0.04

→ Sharing the trunk network does not only save in the number of parameters but even yields better performance

Cf. [Howard, Heinlein, Stinis \(in prep.\)](#)

PACMANN – Point adaptive collocation method for artificial neural networks

Motivation

The number and distribution of the collocation points in the PDE loss \mathcal{L}_{PDE} have a significant influence on the accuracy of the PINN solution. Since the computational work grows with the number of collocation points, the effective placement of the collocation points is important.

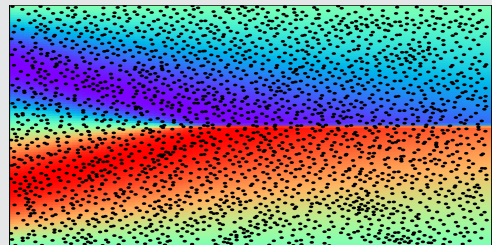
Burger's equation in 1D

Consider the Burger's with one spatial dimension:

$$\frac{\partial u}{\partial t} + u \frac{\partial u}{\partial x} = \nu \frac{\partial^2 u}{\partial x^2}, \quad x \in [-1, 1], \quad t \in [0, 1]$$
$$u(x, 0) = -\sin(\pi x) \quad u(-1, t) = u(1, t) = 0.$$

sampling method	L_2 relative error		mean runtime [s]
	mean	1 SD	
uniform grid	25.9%	14.2%	425
Hammersley grid	0.61%	0.53%	443
random resampling	0.40%	0.35%	423
Residual-based	0.11%	0.05%	450

Implementation based on DeepXDE with PyTorch (v1.12.1)
backend; cf. [Visser, Heinlein, and Giovanardi \(arXiv:2411.19632\)](#)



Similar results in earlier study: [Wu et al. \(2023\)](#)

Overview of Various Sampling Schemes (Not Exhaustive)

Non-adaptive sampling

- **Equispaced uniform grid**
- **Uniformly random sampling**, using a pseudo-random number generator (e.g., PCG-64 [O'Neill \(2014\)](#))
- **Latin hypercube sampling** ([McKay, Beckman, and Conover \(2000\)](#); [Stein \(1987\)](#))

Quasi-random low-discrepancy sequences:

- **Halton sequence** ([Halton \(1960\)](#))
- **Hammersley sequence** ([Hammersley \(1964\)](#))
- **Sobol sequence** ([Sobol' \(1967\)](#))

Adaptive sampling

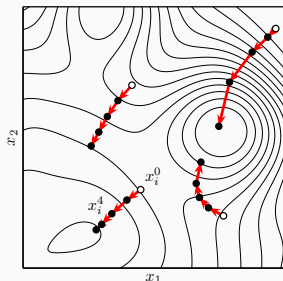
- **Residual-based Adaptive Refinement (RAR)** ([Lu et al \(2021\)](#)): placement of **additional points** in regions with the largest PDE residuals
- **Probability Density Function (PDF)** ([Nabian, Gladstone, and Meidani \(2021\)](#)): randomly resample all points based on a **PDF proportional to the residual**
- **Residual-based Adaptive Distribution (RAD)** ([Wu et al. \(2023\)](#)): **all collocation points are resampled using a PDF based on the residual (nonlinear)**.
- **Residual-based Adaptive Refinement with Distribution (RAR-D)** ([Wu et al. \(2023\)](#)): **sampling of additional collocation points using the PDF used in RAD**
(RAD and RAR-D are based on / extensions of PDF approach)

PACMANN – Point Adaptive Collocation Method for Artificial Neural Networks

In [Visser, Heinlein, and Giovanardi \(arXiv:2411.19632\)](#), the collocation points are updated by solving the **min-max problem**

$$\min_{\theta} \left[\omega_{\text{data}} \mathcal{L}_{\text{data}}(\theta) + \max_{\mathbf{X} \subset \Omega} \omega_{\text{PDE}} \mathcal{L}_{\text{PDE}}(\mathbf{X}, \theta) \right].$$

Different from the other residual-based adaptive sampling methods, the **existing collocation points are moved** using a gradient-based optimizers, such as [gradient ascent](#), [RMSprop](#) ([Hinton \(2018\)](#)), [Adam](#) ([Kingma, Ba \(2017\)](#)), or others.



Algorithm 1: PACMANN with iteration counts P and T and stepsize s

Sample a set \mathbf{X} of N_{PDE} collocation points using a uniform sampling method;

while *stopping criterion not reached* **do**

Train the PINN for P iterations;

for $k = 1, \dots, T$ **do**

Compute squared residual $\mathcal{R}(x_i) = (\mathcal{N}[u](x_i, \theta) - f(x_i))^2$ for all $x_i \in \mathbf{X}$;

Compute gradient $\nabla_{\mathbf{X}} \mathcal{R}(x_i)$ for all $x_i \in \mathbf{X}$;

Move the points in \mathbf{X} according to the chosen optimization algorithm and stepsize s ;

end

Resample points in \mathbf{X} that moved outside Ω based on a uniform probability distribution;

end

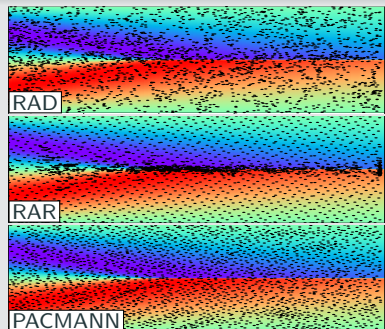
Numerical Results – Burger's Equation in 1D

Varying the optimizer in PACMANN

sampling method	L_2 relative error		mean runtime [s]	hyper parameters	
	mean	1 SD		stepsize s	# steps T
PACMANN–gradient ascent	0.30%	0.17%	436	10^{-6}	1
PACMANN–RMSprop	0.10%	0.03%	442	10^{-6}	10
PACMANN–Adam	0.07%	0.05%	461	10^{-5}	15

Comparison against different methods

sampling method	L_2 relative error		mean runtime [s]
	mean	1 SD	
uniform grid	25.9%	14.2%	425
Hammersley grid	0.61%	0.53%	443
random resampling	0.40%	0.35%	423
RAR	0.11%	0.05%	450
RAD	0.16%	0.10%	463
RAR-D	0.24%	0.21%	503
PACMANN–Adam	0.07%	0.05%	461



Cf. [Visser, Heinlein, and Giovanardi \(arXiv:2411.19632\)](#).

Numerical Results – Poisson Equation in 5D

Furthermore, we show that our method **scales well to higher dimensions**, such as a **Poisson equation in five dimensions**:

$$\begin{aligned}-\Delta u &= f, \quad \text{in } \Omega = [-1, 1]^5, \\ u &= 0, \quad \text{on } \partial\Omega.\end{aligned}$$

Here, f is chosen such that $u = \prod_{i=1}^5 \sin(\pi x_i)$.

Comparison against different methods

sampling method	L_2 relative error		mean runtime [s]
	mean	1 SD	
uniform grid	17.89%	0.94%	742
Hammersley grid	82.08%	3.23%	734
random resampling	11.03%	0.69%	772
RAR	56.84%	4.46%	753
RAD	10.07%	0.75%	851
RAR-D	88.30%	1.53%	774
PACMANN–Adam	5.93%	0.46%	778

Cf. Visser, Heinlein, and Giovanardi ([arXiv:2411.19632](#)).

Numerical Results – Parameter Identification for the Navier–Stokes Equations

Finally, we consider an **inverse problem** involving the **Navier–Stokes equations in two dimensions** of an **incompressible flow past a cylinder** discussed by **Raissi et al. (2019)**:

$$u_t + \lambda_1(uu_x + vu_y) = -p_x + \lambda_2(u_{xx} + u_{yy}), \quad x \in [1, 8] \times [-2, 2], t \in [0, 7],$$

$$v_t + \lambda_1(uv_x + vv_y) = -p_y + \lambda_2(v_{xx} + v_{yy}), \quad x \in [1, 8] \times [-2, 2], t \in [0, 7].$$

Here, (u, v) and p are the velocity and pressure fields. The scalar parameter λ_1 scales the convective term, and λ_2 represents the dynamic (shear) viscosity. The true values of λ_1 and λ_2 are 1 and 0.01.

sampling method	L_2 relative error				mean runtime [s]	
	λ_1		λ_2			
	mean	1 SD	mean	1 SD		
uniform grid	0.05 %	0.01 %	0.72 %	0.43 %	1506	
Hammersley grid	0.08 %	0.04 %	0.89 %	0.52 %	1492	
random resampling	0.12 %	0.05 %	0.65 %	0.46 %	1514	
RAR	0.30 %	0.06 %	1.44 %	0.90 %	1520	
RAD	0.23 %	0.06 %	1.38 %	0.79 %	1583	
RAR-D	0.08 %	0.05 %	0.84 %	0.57 %	1525	
PACMANN–Adam	0.03 %	0.03 %	0.53 %	0.19 %	1559	

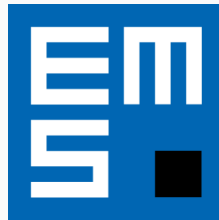
Cf. **Visser, Heinlein, and Giovanardi (arXiv:2411.19632)**.

Annual Meeting of EMS activity group on Scientific Machine Learning

Organizing committee: P.F. Antonietti, S. Pagani, F. Regazzoni, M. Verani (chair), P. Zunino

Scientific committee: Members of the EMS activity group on Scientific Machine Learning

- **Dates:** March 24 – 28, 2025
- **Event:** First Annual Meeting of the EMS-AI Scientific Machine Learning (SciML) activity group
- **Focus:** Bridging mathematics, computer science, and applications in SciML
- **Program Highlights:**
 - 18 Invited Talks
 - 2 Industrial Sessions
 - Poster Session
 - Roundtable Discussion on *Interplay between machine learning, applied mathematics, and scientific computing*; chair: Wil Schilders (ICIAM President)



Deadline for registration: January 31, 2025!

Co-organizers: Victorita Dolean (TU/e), Alexander Heinlein (TU Delft), Benjamin Sanderse (CWI), Jemima Tabbeart (TU/e), Tristan van Leeuwen (CWI)

- **Autumn School** (October 27–31, 2025):
 - [Chris Budd](#) (University of Bath)
 - [Ben Moseley](#) (Imperial College London)
 - [Gabriele Steidl](#) (Technische Universität Berlin)
 - [Andrew Stuart](#) (California Institute of Technology)
 - [Andrea Walther](#) (Humboldt-Universität zu Berlin)
- **Workshop** (December 1–3, 2025):
 - 3 days with plenary talks (academia & industry) and an industry panel
 - Confirmed plenary speakers:
 - [Marta d'Elia](#) (Meta)
 - [Benjamin Peherstorfer](#) (New York University)
 - [Andreas Roskoppf](#) (Fraunhofer Institute)



Centrum Wiskunde & Informatica



Join us for inspiring talks, hands-on sessions, and industry collaboration!

Multilevel FBPINNs

- Schwarz domain decomposition architectures **improve the scalability of PINNs** to large domains / high frequencies, **keeping the complexity of the local networks low**.
- As classical domain decomposition methods, **one-level FBPINNs** are **not scalable to large numbers of subdomains**; **multilevel FBPINNs enable scalability**.

Stacking Multifidelity FBPINNs

- The **combination of multifidelity stacking PINNs with FBPINNs** yields **significant improvements in the accuracy and efficiency** for **time-dependent problems**.

PACMANN Sampling Method

- Adaptive movement of the collocation points along the gradient yields **comparable or better performance compared to state-of-the-art sampling approaches**; standard optimizers can be employed.
- In particular, for **high-dimensional problems**, the **performance is clearly better**.

Thank you for your attention!



Topical Activity
Group
Scientific Machine
Learning

